Generation of a tunable environment for electrical oscillator systems

R. de J. León-Montiel,[1] J. Svozilík,[1,2] and Juan P. Torres[1,3]
[1]*ICFO–Institut de Ciencies Fotoniques, Mediterranean Technology Park, 08860 Castelldefels (Barcelona), Spain*
[2]*Palacký University, RCPTM, Joint Laboratory of Optics, 17. listopadu 12, 77146 Olomouc, Czech Republic*
[3]*Department of Signal Theory and Communications, Campus Nord D3, Universitat Politecnica de Catalunya, 08034 Barcelona, Spain*
(Received 5 February 2014; published 9 July 2014)

Many physical, chemical, and biological systems can be modeled by means of random-frequency harmonic oscillator systems. Even though the noise-free evolution of harmonic oscillator systems can be easily implemented, the way to experimentally introduce, and control, noise effects due to a surrounding environment remains a subject of lively interest. Here, we experimentally demonstrate a setup that provides a unique tool to generate a fully tunable environment for classical electrical oscillator systems. We illustrate the operation of the setup by implementing the case of a damped random-frequency harmonic oscillator. The high degree of tunability and control of our scheme is demonstrated by gradually modifying the statistics of the oscillator's frequency fluctuations. This tunable system can readily be used to experimentally study interesting noise effects, such as noise-induced transitions in systems driven by multiplicative noise, and noise-induced transport, a phenomenon that takes place in quantum and classical coupled oscillator networks.

DOI: 10.1103/PhysRevE.90.012108 PACS number(s): 05.40.Ca, 07.50.Ek, 82.20.Nk, 87.10.Tf

I. INTRODUCTION

For many years, it has been known that fluctuations or noise can play an important role in various effects that take place in different physical, chemical, and biological systems. Some examples of such effects are stochastic resonance [1], noise-induced transitions [2,3], and noise-induced transport, a phenomenon that has been observed in quantum [4,5] and classical [6,7] systems.

Because noise-induced effects are generally described by models where several, albeit reasonable, assumptions are made, an experimental confirmation of these surprising, sometimes counterintuitive, theoretical predictions is certainly most desirable. The verification of predicted noise effects is, in general, most easily achieved on simple experimental systems. As stated in Ref. [2], these systems should exhibit the following features: (i) their time evolution should be well known for deterministic conditions, (ii) their experimental design should not present great technical difficulties, and (iii) variables of the system and the externally introduced noise should be easily controlled. In view of these points, we immediately realize that electrical oscillator circuits are the ideal choice. Indeed, the majority of the experimental studies on noise-induced phenomena have been carried out using electrical circuits [8–11]. Other systems where noise effects have been studied involve surface waves [12], spin waves in ferrites and antiferromagnets [13], and electroconvection in nematic liquid crystals [14].

Most of the experiments mentioned above make use of systems driven by Gaussian white noise. However, it has been shown that systems driven by non-Gaussian noises might also exhibit interesting features, such as shifts in the transition line for noise-induced transitions [15], enhancement of the signal-to-noise ratio in stochastic resonance [16,17], and enhancement of transport efficiency in Brownian motors [18]. Therefore, in order to experimentally investigate new non-Gaussian noise effects, one needs to design a system capable of producing various types of noise bearing different probability distributions.

In this paper, we introduce an experimental setup that performs as a tunable environment for classical electrical oscillators. We test our scheme by implementing the case of a damped random-frequency harmonic oscillator. We have chosen this system because it represents a fundamental tool in statistical physics, which has been extensively used to describe a myriad of physical systems in different research fields [19–23]. The tunability of our system is demonstrated by gradually modifying the statistics of frequency fluctuations, which is managed by properly controlling the mean and variance of the oscillator's frequency distribution. This is particularly relevant because it implies that the system directly introduces fluctuations in the frequency of the signal, which is in contrast to previous experimental studies where fluctuations in the amplitude, rather than frequency, are introduced in the system [11,12].

Because of its high degree of tunability and control, this setup can readily be used to experimentally observe effects of Gaussian [11,24] and non-Gaussian [15] noise-induced transitions, as well as noise-induced transport phenomena [6,7].

II. THE MODEL

We consider a damped random-frequency harmonic oscillator whose temporal evolution reads [25]

$$\frac{d^2x}{dt^2} + \Gamma\frac{dx}{dt} + \omega_0^2[1+\phi(t)]x = 0, \tag{1}$$

where Γ is the damping coefficient, ω_0 is the average frequency of the oscillator, and $\phi(t)$ describes a stochastic Gaussian process with zero average $\langle\phi(t)\rangle = 0$, and a specific autocorrelation function defined by the expression $\langle\phi(t)\phi(t')\rangle = \kappa(t-t')$, where the function $\kappa(t-t')$ defines the type of noise that is considered. For instance, in the case of ideal white noise, the autocorrelation function is defined as $\langle\phi(t)\phi(t')\rangle = 2D\delta(t-t')$, where D denotes the intensity of the noise. A more realistic example is colored noise, where the autocorrelation function is written as $\langle\phi(t)\phi(t')\rangle = (D/\tau_c)\exp(-|t-t'|/\tau_c)$, with τ_c being the correlation time of the stochastic process [26].

Using the cumulant expansion described by Van Kampen [27], Gitterman showed [19,25] that the equation for $\langle x\rangle$, in the fast fluctuations regime, has the form (see the Appendix for a detailed derivation)

$$\frac{d^2\langle x\rangle}{dt^2}+\left(\Gamma+\frac{\omega_0^4}{2\nu^2}c_2\right)\frac{d\langle x\rangle}{dt}+\omega_0^2\left[1-\frac{\omega_0^2}{2\nu}\left(c_1-\frac{\Gamma}{2\nu}c_2\right)\right]\langle x\rangle=0, \tag{2}$$

where $\nu=(\omega_0^2-\Gamma^2/4)^{1/2}$, and the coefficients c_1 and c_2 are defined by

$$c_1=\int_0^\infty\langle\phi(t)\phi(t-\xi)\rangle\sin(2\omega_0\xi)d\xi, \tag{3}$$

$$c_2=\int_0^\infty\langle\phi(t)\phi(t-\xi)\rangle[1-\cos(2\omega_0\xi)]d\xi. \tag{4}$$

Notice that, as pointed out in Ref. [19], the existence of frequency fluctuations in Eq. (1) introduces a noise-induced additional damping and a noise-induced frequency shift to the average signal of the oscillator.

III. EXPERIMENT

A. The setup

The experimental setup that allows us to introduce random frequency fluctuations into a harmonic oscillator model is the following. First, note that one can construct a system governed by Eq. (1) by making use of electrical RLC oscillators (where R stands for resistance, L for inductance, and C for capacitance). In these systems, the charge in the capacitor satisfies the same equation as Eq. (1), where the coefficients Γ and ω_0 are defined by [11]

$$\Gamma=R/L, \tag{5}$$

$$\omega_0=(LC_0)^{-1/2}, \tag{6}$$

with C_0 denoting the average capacitance of the circuit. From Eq. (6) one can see that fluctuations in the frequency of the RLC oscillator can be introduced by randomly switching the values of the capacitance [28].

Random switching of capacitance is performed in the following way: An array of eight capacitors, each with equal capacitance C_a, is connected in parallel to a central capacitor C of a RLC circuit. To produce uncorrelated random switching, the individual capacitors are independently turned *on* and *off* by means of analog switches (NXP-74HC4066N quad bilateral switch), which are driven by independent digital signals provided by an arbitrary function generator (Signadyne digital I/O module SD-PXE-DIO-H0001), as shown in Fig. 1. Because we are interested in designing a Gaussian stochastic process, we program the arbitrary function generator, so each capacitor has the same probability to be on or off, in the same fashion as in a coin-tossing event. It is easy to show that the probability that n capacitors in the array are on satisfies a binomial distribution given by

$$P(n)=\binom{8}{n}\frac{1}{2^8}, \tag{7}$$

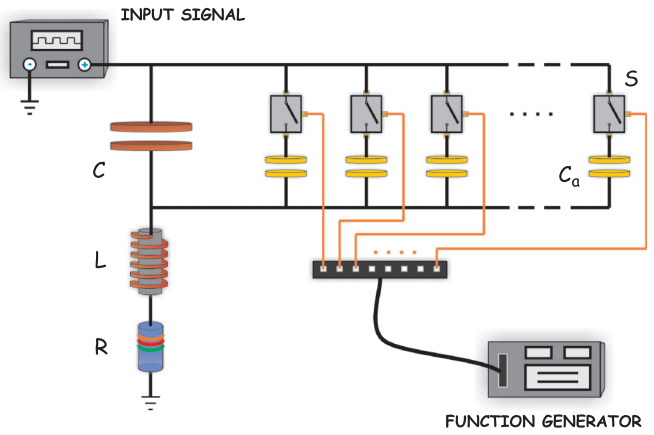

FIG. 1. (Color online) Scheme of the damped random-frequency electrical oscillator consisting of a RLC circuit with central capacitance C, inductance L, and a parasitic resistance R. Frequency fluctuations are achieved by switching on and off individual capacitors C_a by means of analog switches S that are driven by an arbitrary function generator.

where $n=\{0,1,2,\ldots,8\}$. This distribution is defined by a mean value $\langle n\rangle=4$ and a variance $\sigma_b^2=2$. Notice that the binomial distribution described in Eq. (7) is a discrete version of a Gaussian distribution with the same mean and variance, as depicted in Fig. 2. It is important to remark that due to the nonlinear relation between frequency and capacitance [Eq. (6)], when calculating the probability distribution of frequency, a Gaussian distribution is obtained provided that the condition $C_a\ll C$ is satisfied [29].

B. Implementation and results

To test the proposed scheme, we construct a RLC circuit where the central capacitance C is provided by a 1 nF ceramic capacitor, inductance L is provided by a 1.5 mH ferrite core inductor, and resistance R represents parasitic losses within the system. For the random switching of capacitance, we have designed several arrays using different ceramic capacitors with capacitance value $C_a=\{4.7,10,18,33,47,68,100\}$ pF.

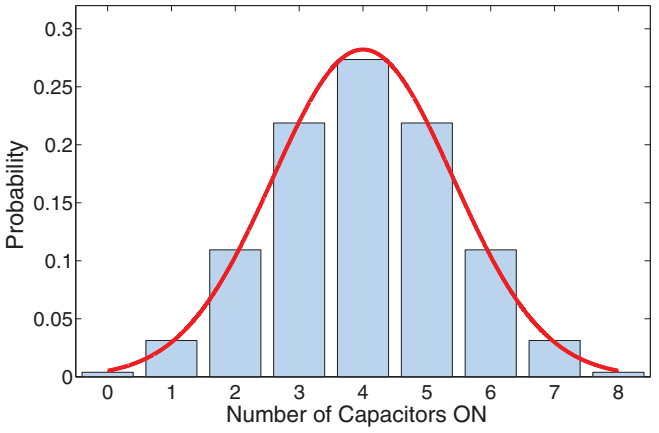

FIG. 2. (Color online) The probability that n capacitors in the array are on follows a binomial distribution, which corresponds to a discretized Gaussian distribution with the same average and variance.

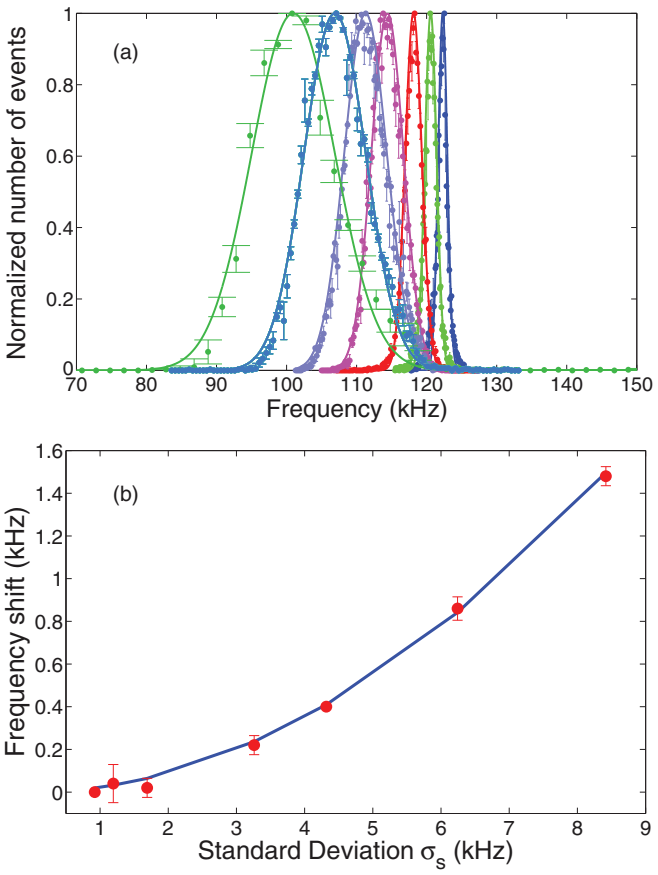

FIG. 3. (Color online) (a) Signal frequency histograms using different capacitor arrays. From left to right: $C_a =$ 100,68,47,33,18,10,4.7 pF. Dotted line: experimental data; solid line: Gaussian fitting. (b) Frequency shift as a function of the standard deviation σ_s. Dotted line: experiment; solid line: theory.

Notice from Fig. 2 that by changing the values of C_a one can modify the variance of the Gaussian distribution, which in turn modifies the statistics of the noise in the system [26].

To guarantee that our system is well described by Eq. (2), we make sure that frequency fluctuations are faster than the characteristic time evolution of the system; that is, they satisfy the fast fluctuations condition [19]. To this end, the digital signals from the arbitrary function generator are set with a time rate $\tau = 650$ ns, which is longer than the response time of the analog switches (400 ns) and much shorter than the temporal evolution window of the measured signal ($t = 100$ μs).

Using the system described above, we have performed the simulation of Eq. (1). To this end, we keep the capacitor C fixed and measure the averaged signal of the oscillator connected to different capacitor arrays. Figure 3(a) shows the histograms of the measured frequency in each case. Histograms are obtained from 50 000 different realizations, and they are normalized to the maximum number of events, where we define the number of events as the number of realizations that have the same value of frequency. Notice that in all cases the probability distribution of the frequency follows a Gaussian distribution whose variance σ_s^2 depends strongly on the value of C_a used in the connected array. This

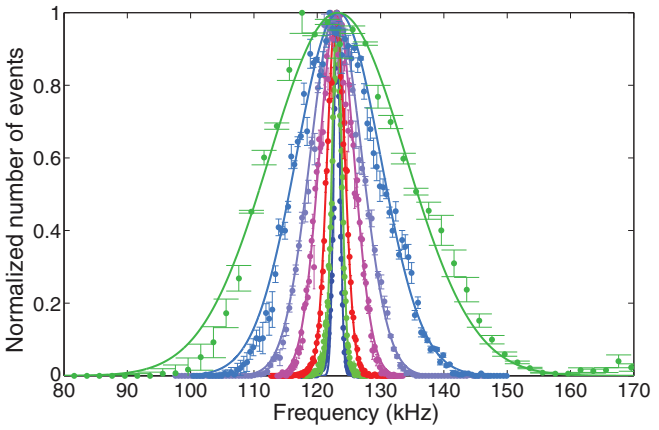

FIG. 4. (Color online) Frequency histograms for different capacitor arrays centered in the same mean frequency $f_0 \simeq 123$ kHz. Dotted line: experimental data; solid line: Gaussian fitting.

implies that this scheme allows us to control the variance of the noise that is introduced in the system. Moreover, notice that by changing the way in which capacitors are turned on and off, one can modify the frequency probability distribution. For instance, a dichotomous-like random frequency could be obtained by switching on and off all capacitors at the same time.

To compare the results obtained in Fig. 3(a) with the theoretical model, we have measured the frequency shift that arises from the influence of frequency fluctuations, as predicted by Eq. (2). Figure 3(b) shows the frequency shift for each capacitor array. We have made use of Eq. (2) and the relation [26] $D = \sigma^2\tau$ to find that the driving noise of our system can be described by a colored-noise-like autocorrelation function of the form

$$\langle\phi(t)\phi(t')\rangle = \frac{\sigma^2}{\omega_0^2}\exp\left(-\frac{|t-t'|}{\tau}\right), \tag{8}$$

where the mean value of the frequency is computed with $C_0 = C + 4C_a$ and the variance of the driving noise is $\sigma^2 = (\eta\sigma_s)^2$, with $\eta = 3.4$. This relation between both variances can be understood as a consequence of the damping term in Eq. (1). The same effect can be found, for instance, in the Ornstein-Uhlenbeck process, where the resulting variance is proportional to the variance of the driving noise due to the presence of a damping term [27].

In general, when simulating noise-induced transport effects, one is interested in keeping the mean frequency of each oscillator fixed while increasing the strength of the noise [4,5,7]. This can be achieved in our system by controlling the values of the central capacitance C and the time duration τ of the digital signals. Figure 4 shows the frequency histograms measured with different capacitor arrays. Notice that by properly controlling the parameters of the system, we are able to center all the probability distributions in the same value of frequency $f_0 \simeq 123$ kHz. This demonstrates the flexibility of our system when modifying the statistical properties of the environmental noise that interacts with the oscillator. The

TABLE I. Experimental parameters used to obtain the histograms shown in Fig. 4.

	C_a (pF)						
	4.7	10	18	33	47	68	100
C (nF)	1.120	1.090	1.053	0.978	0.933	0.840	0.355
τ (ns)	650	650	750	780	800	720	650

parameters of the system used in each case are summarized in Table I.

IV. CONCLUSIONS AND OUTLOOK

In this paper, we have demonstrated a system that performs as a tunable environment for classical electrical oscillators. We have shown its operation by implementing the case of a damped random-frequency oscillator, where perfect agreement with the theoretical model has been obtained. Finally, we have demonstrated the degree of control that one can achieve with this system by gradually modifying the variance of the frequency fluctuations while maintaining a fixed central frequency of oscillation, which is of critical importance when simulating noise-induced energy transfer mechanisms in different scenarios, such as in the case of energy transfer in molecular aggregates.

The high degree of tunability and control of the proposed system can be further used to design various types of noise with different probability distributions. Moreover, it might allow us to study the transition from Markovian to non-Markovian dynamics of open systems. The results reported here represent an important step towards the experimental observation of Gaussian and non-Gaussian noise-induced transitions and noise-induced transport effects.

ACKNOWLEDGMENTS

We thank A. Vallés, L. J. Salazar Serrano, Y. de Icaza Astiz, D. Mitrani, and J. C. Cifuentes for valuable discussions. This work was supported by the projects funded by the government of Spain FIS2010-14831 and Severo Ochoa. This work has also been partially supported by Fundacio Privada Cellex Barcelona. J.S. acknowledges Project No. PrF-2013-006 of IGA Palacky University Olomouc, and Grants No. CZ.1.07/2.3.00/30.0004 and No. CZ.1.07/2.3.00/20.0058 of MŠMT ČR.

APPENDIX: DERIVATION OF THE AVERAGED AMPLITUDE EQUATION OF A DAMPED RANDOM-FREQUENCY HARMONIC OSCILLATOR

Let us consider the equation for a damped random-frequency harmonic oscillator,

$$\frac{d^2x}{dt^2} + \Gamma\frac{dx}{dt} + \omega_0^2[1 + \alpha\phi(t)]x = 0, \tag{A1}$$

where Γ is the damping coefficient, ω_0 is the average frequency of the oscillator, and $\phi(t)$ is a dimensionless stochastic variable with zero average $\langle\phi(t)\rangle = 0$, and an autocorrelation function satisfying $\langle\phi(t_1)\phi(t_2)\rangle \to 0$ for any two time points t_1, t_2 such that $|t_2 - t_1| > \tau_c$, where τ_c is the correlation time of the stochastic process. To simplify the derivation of Eq. (2), and for consistency with Ref. [27], we have included in Eq. (A1) the parameter α, which represents the strength of the stochastic fluctuations.

In order to solve Eq. (A1), we first transform it into a set of first-order differential equations

$$\frac{d}{dt}X = (M_\mathrm{d} + M_\mathrm{s})X, \tag{A2}$$

where

$$X = \begin{bmatrix} x(t) \\ \dot{x}(t) \end{bmatrix}, \tag{A3}$$

$$M_\mathrm{d} = \begin{bmatrix} 0 & 1 \\ -\omega_0^2 & -\Gamma \end{bmatrix}, \tag{A4}$$

$$M_\mathrm{s} = \begin{bmatrix} 0 & 0 \\ -\alpha\omega_0^2\phi(t) & 0 \end{bmatrix}. \tag{A5}$$

Here, the matrices M_d and M_s represent the deterministic and stochastic evolution of the oscillator, respectively, and $\dot{x}(t)$ stands for the time derivative of the oscillator's amplitude x.

In the matrix representation, it is easy to show that the equation for the deterministic evolution of the oscillator, i.e., $\dot{X}_\mathrm{d} = M_\mathrm{d}X_\mathrm{d}$, has the solution

$$X_\mathrm{d}(t) = U_\mathrm{d}(t)X_\mathrm{d}(0), \tag{A6}$$

where

$$U_\mathrm{d}(t) = \exp\left(-\frac{\Gamma}{2}t\right)\begin{bmatrix} \cos(\nu t) + (\Gamma/2\nu)\sin(\nu t) & \sin(\nu t)/\nu \\ -\omega_0^2\sin(\nu t)/\nu & \cos(\nu t) - (\Gamma/2\nu)\sin(\nu t) \end{bmatrix}. \tag{A7}$$

Notice that the presence of damping in the harmonic oscillator produces a frequency shift that is given by $\nu = \sqrt{\omega_0^2 - \Gamma^2/4}$.

Now, we make use of Eq. (A7) to perform the transformation

$$X(t) = U_\mathrm{d}(t)\tilde{X}(t), \tag{A8}$$

which, when substituted into Eq. (A2), allows us to write

$$\frac{d}{dt}\tilde{X} = \alpha U_\mathrm{d}(-t)\,M_\mathrm{s}(t)\,U_\mathrm{d}(t)\,\tilde{X}(t). \tag{A9}$$

Then, we iteratively solve Eq. (A9) to find that the average of $\tilde{X}$ is written as

$$\langle \tilde{X}(t)\rangle = \langle \tilde{X}(0)\rangle + \alpha^2 \int_0^t dt_1 \int_0^\infty dt_2 \langle U_{\rm d}(-t_1)\, M_{\rm s}(t_1)\, U_{\rm d}(t_1-t_2)\, M_{\rm s}(t_2)\, U_{\rm d}(t_2)\rangle \langle \tilde{X}(0)\rangle. \tag{A10}$$

Notice that the linear term with α disappears since $\langle M_{\rm s}(t)\rangle = 0$. In writing Eq. (A10), we have considered only the contributions up to α^2, which is an approximation that is valid as long as the condition $\alpha\tau_c \ll 1$ is satisfied. In addition, we have assumed that the correlation time τ_c is much shorter than the integration time, so we can take $\langle \tilde{X}(t)\rangle \to \langle \tilde{X}(0)\rangle$ and integrate to infinity in the second term of Eq. (A10).

We now perform the time derivative of Eq. (A10) to obtain

$$\frac{d}{dt}\langle \tilde{X}(t)\rangle = \alpha^2 \int_0^\infty d\xi \langle U_{\rm d}(-t)\, M_{\rm s}(t) U_d(\xi)\, M_{\rm s}(t-\xi)\, U_{\rm d}(t-\xi)\rangle \langle \tilde{X}(0)\rangle, \tag{A11}$$

where the substitutions $\xi = t_1 - t_2$ and $t = t_1$ are used. Inverse transformation of Eq. (A11), by means of Eq. (A8), then gives

$$\frac{d}{dt}\langle X(t)\rangle = \left[M_{\rm d} + \alpha^2 \int_0^\infty d\xi \langle M_{\rm s}(t) U_{\rm d}(\xi)\, M_{\rm s}(t-\xi)\, U_{\rm d}(-\xi)\rangle\right]\langle X(t)\rangle. \tag{A12}$$

Using Eqs. (A5) and (A7), we can readily find that the expression inside the integral of Eq. (A12) is written as

$$\langle M_{\rm s}(t) U_{\rm d}(\xi)\, M_{\rm s}(t-\xi)\, U_{\rm d}(-\xi)\rangle = \omega_0^4 \langle \phi(t)\,\phi(t-\xi)\rangle \begin{Bmatrix} 0 & 0 \\ [\sin(\nu\xi)/\nu][\cos(\nu\xi) - (\Gamma/2\nu)\sin(\nu\xi)] & -\sin^2(\nu\xi)/\nu^2 \end{Bmatrix}. \tag{A13}$$

Finally, by substituting Eq. (A13) into Eq. (A12) and transforming the set of two first-order equations to a single second-order differential equation, Eq. (2) is obtained.

[1] L. Gammaitoni, P. Hänggi, P. Jung, and F. Marchesoni, Rev. Mod. Phys. **70**, 223 (1998).

[2] W. Horsthemke and R. Lefever, *Noise-Induced Transitions: Theory and Applications in Physics, Chemistry, and Biology* (Springer, Berlin, 1984).

[3] C. Van den Broeck, J. M. R. Parrondo, and R. Toral, Phys. Rev. Lett. **73**, 3395 (1994).

[4] P. Rebentrost, M. Mohseni, I. Kassal, S. Lloyd, and A. Aspuru-Guzik, New J. Phys. **11**, 033003 (2009).

[5] M. Plenio and S. Huelga, New J. Phys. **10**, 113019 (2008).

[6] P. Hänggi and F. Marchesoni, Rev. Mod. Phys. **81**, 387 (2009).

[7] R. de J. León-Montiel and J. P. Torres, Phys. Rev. Lett. **110**, 218101 (2013).

[8] T. Kawakubo, S. Kabashima, and Y. Tsuchiya, Progr. Theor. Phys. **64**, 150 (1978).

[9] S. Kabashima and T. Kawakubo, Phys. Lett. A **70**, 375 (1979).

[10] S. Kabashima, S. Kogure, T. Kawakubo, and T. Okada, J. Appl. Phys. **50**, 6296 (1979).

[11] R. Berthet, A. Petrossian, S. Residori, B. Roman, and S. Fauve, Physica D (Amsterdam, Neth.) **174**, 84 (2003).

[12] S. Residori, R. Berthet, B. Roman, and S. Fauve, Phys. Rev. Lett. **88**, 024502 (2001).

[13] V. V. Zautkin, B. I. Orel, and V. B. Cherepanov, Zh. Eksp. Teor. Fiz. **85**, 708 (1983) [Sov. Phys. JETP **58**, 414 (1983)].

[14] T. John, R. Stannarius, and U. Behn, Phys. Rev. Lett. **83**, 749 (1999).

[15] H. S. Wio and R. Toral, Physica D (Amsterdam, Neth.) **193**, 161 (2004).

[16] M. A. Fuentes, R. Toral, and H. S. Wio, Physica A (Amsterdam, Neth.) **295**, 114 (2001).

[17] F. J. Castro, M. N. Kuperman, M. Fuentes, and H. S. Wio, Phys. Rev. E **64**, 051105 (2001).

[18] S. Bouzat and H. S. Wio, Eur. Phys. J. B **41**, 97 (2004).

[19] M. Gitterman, *The Noisy Oscillator: The First Hundred Years, from Einstein until Now* (World Scientific, Singapore, 2005).

[20] R. Graham, M. Höhnerbach, and A. Schenzle, Phys. Rev. Lett. **48**, 1396 (1982).

[21] A. Ishimaru, *Wave Propagation and Scattering in Random Media* (IEEE Press, Piscataway, NJ, 1997).

[22] M. Turelli, Theor. Popul. Biol. **12**, 140 (1977).

[23] H. Takayasu, A.-H. Sato, and M. Takayasu, Phys. Rev. Lett. **79**, 966 (1997).

[24] M. Gitterman and D. A. Kessler, Phys. Rev. E **87**, 022137 (2013).

[25] M. Gitterman, Physica A (Amsterdam, Neth.) **352**, 309 (2005).

[26] C. Laing and G. J. Lord, *Stochastic Methods in Neuroscience* (Clarendon, Oxford, 2008).

[27] N. G. Van Kampen, *Stochastic Processes in Physics and Chemistry* (Elsevier, Amsterdam, 2007).

[28] For the sake of simplicity, we have selected a random switching of the capacitance. However, one can always choose to randomly change the values of the inductance. By doing this, one adds more complexity to the system since the damping coefficient would randomly fluctuate as well.

[29] K. Jacobs, *Stochastic Processes for Physicists: Understanding Noisy Systems* (Cambridge University Press, Cambridge, 2010).